Available online at www.sciencedirect.com

ScienceDirect

Biomedical Journal

journal homepage: www.elsevier.com/locate/bj

Original Article

The spontaneous immortalization probability of mammalian cell culture strains, as their proliferative capacity, correlates with species body mass, not longevity

Matteo Perillo [a,*], *Angela Punzo* [a], *Cristiana Caliceti* [a], *Christian Sell* [b], *Antonello Lorenzini* [a]

[a] *Department of Biomedical and Neuromotor Sciences, University of Bologna, Italy*
[b] *Department of Biochemistry & Molecular Biology, Drexel University College of Medicine, Philadelphia, PA, USA*

ARTICLE INFO

Article history:
Received 17 March 2023
Accepted 29 April 2023
Available online 5 May 2023

Keywords:
Cell culture immortalization
Replicative senescence
Longevity
Body mass
Partial correlation
Phylogenetic regression

ABSTRACT

Background: The *Peto's paradox* consists in the observation that individuals from long-lived and large animal species do not experience a higher cancer incidence, despite being exposed for longer time to the possibility of accumulating mutations and having more target cells exposed to the phenomenon. The existence of this paradox has been recently confirmed (Vincze et al., 2022). Concurrently, robust evidence has been published that longevity involves a convergent evolution of cellular mechanisms that prevent the accumulation of mutations (Cagan et al., 2022). It remains unclear which cellular mechanisms are critical to allow the evolution of a large body mass while keeping cancer at bay.
Methods: Adding to existing data linking cellular replicative potential and species body mass (Lorenzini et al., 2005), we have grown a total of 84 skin fibroblast cell strains from 40 donors of 17 mammalian species and analyzed their Hayflick's limit, i.e., their senescent plateau, and eventual spontaneous immortalization escape. The correlation of immortalization and replicative capacity of the species with their longevity, body mass and metabolism has been assessed through phylogenetic multiple linear regression (MLR).
Results: The immortalization probability is negatively related to species body mass. The new evaluation and additional data about replicative potential strengthen our previous observation, confirming that stable and extended proliferation is strongly correlated with the evolution of a large body mass rather than lifespan.
Conclusion: The relation between immortalization and body mass suggests a need to evolve stringent mechanisms that control genetic stability during the evolution of a large body mass.

* *Corresponding author*. Department of Biomedical and Neuromotor Sciences, University of Bologna, Via Zamboni, 33, Bologna 40126, Italy.
E-mail address: matteo.perillo2@unibo.it (M. Perillo).
Peer review under responsibility of Chang Gung University.
https://doi.org/10.1016/j.bj.2023.100596

At a glance commentary

Scientific background on the subject

Peto's paradox suggests that species with high body mass must have evolved protective mechanisms against cancer. One of the hallmarks of cancer is enabling replicative immortality. The probability of spontaneous immortalization of primary normal cultures varies substantially across species.

What this study adds to the field

We observe a clear relationship between immortalization probability and body mass of species. This result suggests that evolving a large body mass requires the evolution of more stringent mechanisms to control cells proliferation, thus protecting the species from cancer.

Introduction

Cellular senescence was first observed by Hayflick and Moorhead, who documented the limited replicative capacity of normal cells in culture [1]. Initially identified in cell culture, cells with characteristics of senescence are present in aged tissues, and targeting these senescent cells has been found to improve late-life function in animal models [2,3], although senescence may also play a functional role during embryonic development and wound healing [4,5], and we have proposed a positive role in contributing to species longevity by acting during development [6].

Cells that evade senescence acquire the ability to proliferate indefinitely, a process known as immortalization. This phenomenon may also cause cells to avoid senescence entirely, by displaying a culture's growth curve where the senescent plateau is not observed. Immortalization can be spontaneous or induced through genetic manipulation: impairment of cell cycle checkpoints, reactivation or up-regulation of telomerase, up-regulation of oncogenes, and viral infection [7,8]. Immortalization of human cells is considered a hallmark of human cancer and a central aspect of the so called "transformed phenotype" which is a descriptor of a cell that has the capacity to form tumour metastases [9]. Genetic instability is a second hallmark of cancer that may be linked to immortalization as the process is known to be accelerated by the inactivation of key regulators of cell cycle progression.

The capacity for immortalization depends upon multiple factors, among which genetic instability may be prominent, i.e., the tendency to accumulate mutations, chromosomal abnormalities and/or the acquisition of aneuploidy; however, embryonic stem cells are capable of unlimited symmetric divisions while maintaining a stable diploid karyotype. Thus, genomic maintenance is an important housekeeping function; however, it is reasonable to hypothesize that genes related to genome maintenance are subject to evolutionary pressure and may be influenced by the evolution of body size and longevity. Multiple studies indicate the existence of convergent adaptations in cellular protective mechanisms during the evolution of large body mass and longevity (reviewed by Croco et al. [10]). For example, we have found an inverse relationship between species body mass and micronuclei formation [11], and also between species body mass and spindle assembly checkpoint tolerance [12], but a positive correlation between longevity and non-homologous end joining (NHEJ) [13,14], as well as between longevity and stress-induced senescence [6].

The Peto's paradox is based on the concept that cancers are driven by cell intrinsic mechanisms, a concept which inherently disregards organismal level metabolic and hormonal influences as well as immunosurveillance mechanisms, thus representing a relatively simplified view of cancer development. Nonetheless, if one considers cells from all species similarly susceptible to cancer causing insults due to intrinsic and extrinsic sources, then species with larger body mass and longer lifespan should be more susceptible to cancer based on the higher number of cells (in larger animals) and to the longer time available to accumulate insults (in longer-lived species) [15].

Available data show that there is no correlation between body mass and cancer risk across species, confirming *Peto's paradox* [16], suggesting that the evolution of larger body masses requires the evolution of increasingly efficient cancer suppression mechanisms. The same work reports that there is no correlation between longevity and cancer risk across species, suggesting that the evolution of longevity also requires the evolution of increasingly efficient cancer suppression mechanisms. If one postulates that cancer is fundamentally the result of the accumulation of several mutations, somatic mutation rates should inversely correlate with species longevity, a hypothesis that has recently found strong experimental support [17].

In order to better understand the relationships between longevity, body mass, and genetic stability, we have expanded and reanalysed our previous dataset on replicative capacity that we published in 2005 [18]. Now we have added more species information regarding proliferative capacity and previously unreported spontaneous immortalization frequency for 17 mammalian species. Using the approach of Cagan et al. [17], we also assess the relation between basal metabolic rate (BMR) and replicative and immortalization capacities across species.

Material, methods, and data

Measurement of replicative capacity

In this study, the replicative capacity of cell strains has been measured through the computation of their population doubling (PD) level, as described in Cristofalo & Charpentier [19]. PD corresponds to the number of times a cell population doubles since the establishment of the primary culture in vitro.

Proliferative capacity (also referred to as the *Hayflick's limit*) is determined through the observation of a plateau or an inflection point in the cumulative growth curve of the cell strain. The replicative capacity of each cellular strain has been evaluated on a weekly base. If during a 4-week period, the culture was not doubling (i.e., ΔPD<1 over 4 weeks) the cellular strain was considered to have reached senescence. In addition to the analysis of the growth curve we monitored cellular morphology and measured cellular volume using a Z2 Beckman Coulter Counter. These methods are more extensively described in Ref. [18]. To obtain the species average of proliferative potential we have first averaged the PDs across the strains derived from the same donor and then averaged across all the donors of the same species.

Estimation of probability of immortalization

To estimate the probability of immortalization (IP) for the cell strains of each species, the frequency of immortalization (IF) has been measured for each individual as the ratio between the number of immortalizing strains and the total number of strains cultured; then, the species grand means have been computed by averaging the IF across individuals of the same species. In order to be sure to observe the overgrowth of an immortal subpopulation among a senescent culture, we kept observing and if necessary subculturing, a strain that had reached senescence (by the criterium above described) at least for an additional 4-weekd period. As done for the determination of senescence describe above, the estimation of an immortalization event was also based on cellular morphology (transition from a senescent morphology back to an early-passage morphology), measurement of cellular volume using a Z Beckman Coulter Counter (since volume usually decreases during immortalization), and, in a subset of strains, karyotype spreads to assess chromosome instability (considering immortalization a more unstable status).

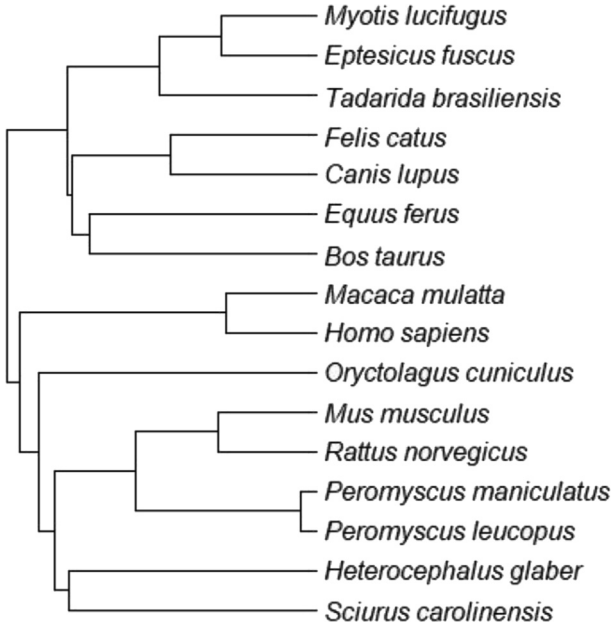

Fig. 1 Phylogenetic tree of the species analysed in the study. 100 trees have been generated using the tool available at https://vertlife.org/phylosubsets/, and the most representative tree has been used for the analysis.

Cell strains and culture conditions.

In this study, data about replicative senescence and immortalization capacity of 107 cell strains from 40 donors of 17 different species have been analyzed. The phylogenetic tree shown in Fig. 1 provides an outline of the evolutionary relation between the species included in the study. The presence of data coming from different donors allows to control for the intraspecies variability for both proliferative and immortalization capacity.

Data were collected in the laboratory of Dr. Cristofalo at the Lankenau Institute for Medical Research, Philadelphia PA (US), and in the one of Dr. Lorenzini at the Department of Biomedical and Neuromotor Sciences, University of Bologna (IT). Cells have been cultivated according to the standard procedure introduced by Cristofalo & Charpentier [19], except for the addition of antibiotics and antimycotics: 100 mg/mL of streptomycin, 0.25 mg/mL of amphotericin B and 100 Ul/mL of penicillin have been added to the culture media.

89 cellular cultures have been instituted through multiple biopsies extracted from the skin of each animal and 31 cultures were obtained from the Coriell Institute for Medical Research (CIMR, Camden NJ, USA). Most of the animals were young or adults. Data from five strains, coming from two 6-months-old rats, were already published in a study by Pignolo et al. [20]; 18 strains, coming from 11 humans, were published in a study by Cristofalo et al. [21]. Such species have been considered only for the analysis of proliferative capacity.

Most of the strains have been derived using the procedure reported by Pignolo et al. [20]. Different procedures have been followed for cellular cultures of big brown bat (*eptesicus fuscus*) and for the strains obtained from the CIMR. The biopsies of big brown bat have been treated for a night with a solution of trypsin at 0.25%, after which collagenase has been added and the biopsies have been put at 37° for 30 min. For the harmonization of data derived directly from the CIMR see the approach described in Appendix 1 (subsection "Details about the cultured cell strains").

Other variables

Maximum longevity of the species (expressed in years), average adult body mass (expressed in grams) and BMR (expressed in watt) have been retrieved from AnAge. AnAge is a "curated database of ageing and life history in animals, including extensive longevity records" [22]. For the body mass, the value "adult weight" from the section "Life history traits" has been taken from the database.

Data about two breeds of *canis lupus familiaris* (rottweilers and beagles) have been collected. Maximum longevity and average adult body mass for each breed have been taken from sources other than AnAge ([23,24]; American Kennel Club website – link: https://www.akc.org/). For each breed, the average among the statistics for male and female specimens has been computed. The average mass, longevity, PD and IF between the two breeds has been used for the analysis.

The value of BMR was not available on AnAge for five species. For three of them (*canis lupus*, *felis catus*, and *macaca mulatta*) the value has been taken from the scientific literature [25], while the others (*equus ferus caballus* and *gorilla*) have been excluded from the analyses in which the BMR was considered. Since the almost perfect correlation between ln (BMR) and ln (mass) (R2 = 0.99) could have caused multicollinearity issues, the creation of a new variable, *Residual BMR* (BMRr), was necessary. The BMRr has been derived following the definition of [17]: the BMRr values are equal to the residuals of the simple linear regression between ln (BMR) and ln (mass).

Statistical analysis

This work extends our previous analysis, where the maximal cell replicative capacity (measured as PD) across species was found to be positively correlated with the body mass of those species and uncorrelated with their longevity [18].

In the present work, the same analysis has been repeated considering more species (more details in Section "Replicative capacity measurement") and including BMRr as candidate explanatory variable for the PD. Moreover, an analogous analysis has been performed to quantify the correlation of the IP of the cell strains across species with body mass, maximum longevity, and BMRr. The whole statistical analysis has been performed using the software R and the RStudio GUI (https://www.R-project.org/, http://www.posit.co/).

Multiple linear regression (MLR) models have been fitted to the collected data, measuring the correlation of proliferative or immortalizing capacities of the cells (dependent/response variables) with longevity, body mass and BMRr (independent/explanatory variables). Performing an MLR allows to quantify the correlation of each independent variable with the dependent variable, net of the relation of the latter with any other independent variable included in the model. In this case, for example, it has allowed us to assess the relationship between longevity and proliferative or immortalizing capacity controlling for mass (and vice versa).

For the regression with PD as a dependent variable, the standard linear model has been fitted using the R function *lm*. In agreement to what has been previously done by Ref. [26], the values of longevity, mass and PD have been log-transformed prior to the analysis. The resulting regression equation is:

$$\ln(PD) = \beta_0 + \beta_1 * \ln(mass) + \beta_2 * \ln(long) + \beta_3 * \mathrm{BMRr}$$

where *long* is the maximum longevity of the species and *mass* is their average adult body mass.

For the regressions with IP as a dependent variable, the quasi-binomial logistic model has been fitted using the R function *glm*. Also in this case, the values of longevity and mass have been log-transformed. The resulting regression equation is:

$$IP = \frac{1}{1 + e^{-[\beta_0 + \beta_1 * \ln(mass) + \beta_2 * \ln(long) + \beta_3 * \mathrm{BMRr}]}}$$

The correlation between each independent variable and the dependent variable in both models has been assessed using the *t-values*. In a MLR each t-value is a measure of the *partial correlation* between one independent variable and the dependent variable, net of the effect of the other independent variable(s). Based on these values, *t-tests* are conducted to check the null hypothesis of "no correlation between the independent variable and the dependent variable".

Moreover, the *Akaike Information Criterion* (AIC) and *Bayesian Information Criterion (BIC)* have been used to assess the performance of the models about PD, while the goodness of fit of the models about IP has been assessed through the *analysis of deviance* (F test) on each model. It is important to highlight that all these techniques do not allow to compare models fitted on different sets of observations. Hence, to compare the models with BMRr as regressor and the ones without it, it has been necessary to refit the models without BMRr on the subset of species for which the BMR was available.

The *"crude" pairwise linear correlations* between log-transformed body mass, longevity, BMR and PD have been computed using the *Pearson correlation coefficient*, r. Also the *partial correlation* between each independent variable and each the dependent variable, controlling for the other independent variables, has been computed.

To measure the partial correlation $r_{xy,z}$ between two variables x and y net of a third variable z (controlling variable) the following procedure has been used. Two regression models are fitted, one analyzing the relation among z and x and the other analyzing the relation among z and y. The correlation among the residuals of these two models is the partial correlation between x and y controlling for z. This procedure allows to produce the *residual–residual plot*, providing a visual representation of the relation between x and y controlling for z. If the crude correlations (r_{xy}, r_{xz}, and r_{yz}) are available, the partial correlation can be equivalently computed as follows:

$$r_{xy,z} = \frac{r_{xy} - (r_{xz} * r_{yz})}{\sqrt{(1 - r_{xz})^2 * (1 - r_{yz})^2}}$$

In this study, the function *pcor* from the R package *ppcor* has been used to compute the partial correlations between:

- PD and mass, controlling for longevity and BMRr;
- PD and longevity, controlling for mass and BMRr;
- PD and BMRr, controlling for mass and longevity.

The regression models described above have also been refitted considering the phylogenetic relation between the species. This has been done using the R function *gls* from the package *nlme*, which allows to perform *phylogenetic regression*, i.e., a regression in which the correlation matrix of the residuals is proportional to a correlation matrix derived from the phylogenetic tree of the species under analysis. The scaling coefficient for the correlation matrix, which must be between 0 and 1, is called *Pagel* λ: if it is equal to 0, there is no phylogenetic signal in the residuals; if it is equal to 1 there is the maximum possible amount of phylogenetic signal in the residuals, and the model is equivalent to a *Brownian motion* model. To perform the phylogenetic regression, 100 phylogenetic trees have been generated by the online tool developed by VertLife (available at https://vertlife.org/phylosubsets/). They have been imported on R using the package *ape*, and the most representative tree has been selected using three

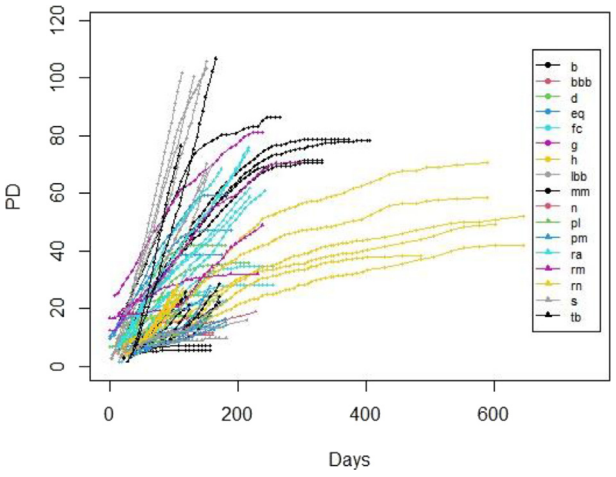

Fig. 2 Growth curve of all the cell strains. Each color/symbol combination corresponds to a species. The species codes are available in Appendix 1 (Table A1).

methods: *average*, *median* and *consensus*. The same tree, displayed in Fig. 1, was found to be representative with all the methods. Based on such tree a correlation matrix has been generated; it has been used as input for the function *gls*, together with 500 possible values of *Pagel* λ.

For the models examining the IP, since the *gls* function does not allow to perform logistic regression, a gaussian regression with *logit*(*IP*) as response variable has been performed. The logit transformation has been performed using the *logit* function from the R package *car*, which remaps the 0 to 0.025 and the 1 to 0.975.

Table 2 The raw pairwise correlations between mass, longevity, PD (log-transformed) and "residual BMR(BMRr)" and the partial correlation between PD and each independent variable, controlling for the others. The correlation between PD and mass is the strongest, but also the correlation of PD with the other two regressors is moderately strong. The correlation between BMRr and the other two independent variable is slightly positive. The partial correlation between PD and mass (both log-transformed) and between PD (log-transformed) and BMRr is statistically significant; the partial correlation between PD and longevity (both log-transformed) is not. This means that, for fixed mass and BMR, a change in longevity is not correlated with a change in PD.

Var 1	Var 2	Control	Correlation	*p-val*
ln (mass)	ln (long)	-	0.54	0.024
ln (mass)	BMRr	-	0.15	0.614
ln (long)	BMRr	-	0.6	0.031
ln (PD)	ln (mass)	-	0.83	0.0001
ln (PD)	ln (mass)	ln (long), BMRr	0.82	0.002
ln (PD)	ln (long)	-	0.68	0.006
ln (PD)	ln (long)	ln (mass), BMRr	0.07	0.829
ln (PD)	BMRr	-	0.47	0.042
ln (PD)	BMRr	ln (mass), ln (long)	0.63	0.039

Results

We have grown 84 cell strains from 17 species and determined their proliferative capacity and immortalization frequency as specified in the Methods section; all the growth curves are shown in Fig. 2. In Appendix 1 we have also reported the growth curve for each strain and, when available, the one on average cellular diameter, as well as some micrographs of the

Table 1 The values of adult average body mass, maximum longevity, basal metabolic rate (BMR), proliferative capacity, immortalization frequency, number of donors and number of lines for each species.

Species	Adult average body mass (g)	Max longevity (years)	BMR (W)	Prol Capacity (PD; SE)	Immort Freq	Number of donors; lines[a]	
Myotis lucifugus	10.0	34.00	0.051	27.86 (NA)	1.00	2	7
Tadarida brasiliensis	12.5	12.00	0.117		1.00	1	2
Mus musculus	20.5	4.00	0.271	8 (1.1)	0.83	3	11
Peromyscus maniculatus	20.5	8.30	0.219	10.74 (3.14)	1.00	2	6
Eptesicus fuscus	23.0	19.00	0.113	13.61 (2.68)	1.00	2	2
Peromyscus leucopus	23.0	7.90	0.213	8.08 (NA)	1.00	1	3
Heterocephalus glaber	35.0	31.00	0.128	15.72 (NA)	1.00	1	3
Rattus norvegicus	300.0	3.80	2.000	19 (NA)	1.00	5	13
Sciurus carolinensis	533.0	23.60	2.062	9.73 (NA)	0.66	1	3
Oryctolagus cuniculus	1800.0	13.00	7.395		1.00	1	5
Felis catus	3900.0	30.00	7.360	24.29 (9.95)	0.33	3	6
Macaca mulatta	8235.0	40.00	10.030	40.27 (26.9)	0.33	3	3
Canis lupus familiaris (agg.)	29250.0	12.1	42.390	20.12 (11.38)	0.00	3	9
\\(Beagle)	13600.0	15.25		29.9 (NA)	0.00	1	4
\\(Rottweiler)	44900.0	9.00		10.34 (2.04)	0.00	2	5
Homo sapiens	62035.0	90.00[b]	82.780	42.1 (7.55)	0.00	13	24
Gorilla	139842.0	60.10		81.37 (NA)		1	1
Equus ferus caballus	300000.0	57.00		48.47 (10.46)	0.00	3	3
Bos taurus	750000.0	20.00	306.770	77.41 (2.33)	0.00	2	5

[a] Some of the strains could not be considered in the analysis of replicative capacity and/or immortalization frequency. See Appendix 1 for more information.

[b] The maximum recorded longevity for humans is 122.5 years, but it has been lowered to 90 years to adjust for the unfairness in the comparison with other species, due to the fact that for human a considerably larger sample to draw statistics from is available.

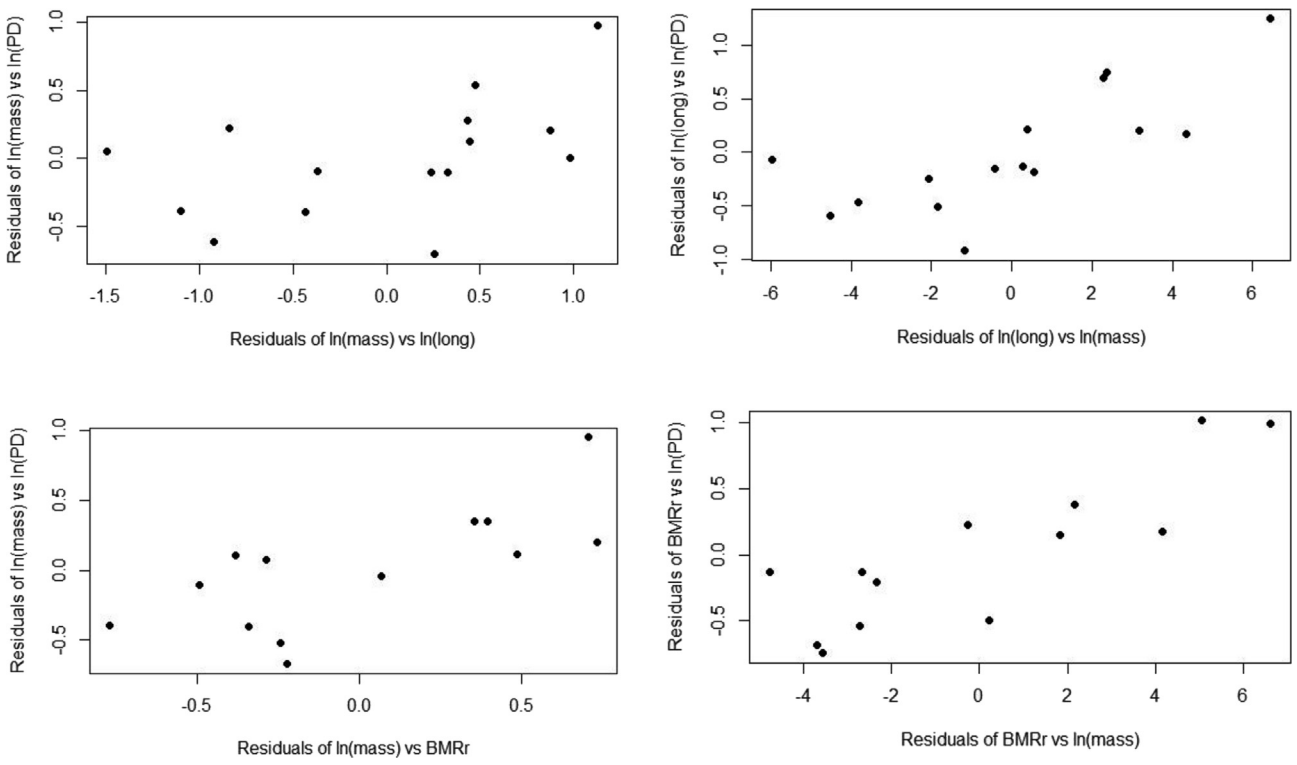

Fig. 3 Residual–residual plots showing the partial correlations in the regression models "ln (PD) vs ln (mass) and ln (long)" and "ln (PD) vs ln (mass) and BMRr". The top-left subplot displays the partial correlation between ln (long) and ln (PD), controlling for ln (mass); the top-right subplot displays the partial correlation between ln (mass) and ln (PD), controlling for ln (long). The bottom-left subplot displays the partial correlation between BMRr and ln (PD), controlling for ln (mass); the bottom-right subplot describes the partial correlation between ln (mass) and ln (PD), controlling for BMRr.

cells taken during the culture, and some histograms about the chromosome number distribution. We have integrated such data with 23 more strains previously published [20,21]. The species-wise averages of the data that we have collected, i.e., proliferative capacity (PD) and immortalization frequency (IF) are presented in Table 1, together with the other variables used in the analysis.

Proliferative capacity

As an exploratory analysis, the pairwise crude correlations and partial correlations between the log-transformed mass, longevity, and PD have been computed. As shown in Table 2, body mass, longevity, and BMRr are correlated with PD, with mass having the strongest correlation. The known correlation between longevity and body mass is confirmed by the data, suggesting that mass may act as a confounder in the relation between longevity and PD, as observed in our previous analysis [18]. Also, the partial correlation of PD with each independent variable controlling for the other two independent variables has been measured, obtaining the results shown in Appendix 1, which can be synthesized as follows: mass and BMRr are correlated with PD also after the control, while longevity is not. Fig. 3 contains the residual–residual plots giving a graphical representation of the partial correlations between mass and PD controlling for longevity and between longevity and PD controlling for mass, as well as the relation between mass and PD net of BMRr, and between BMRr and PD net of mass.

Coherently with what observed measuring the partial correlations, the analysis of AIC and BIC of the MLR models fitted (summarized in Table 3), suggests that the best model to explain the variability of PD between the species is the one which includes mass and BMRr as regressors. The estimated regression equation is the following:

$$\ln(PD) = 2.087 + 0.131*\ln(mass) + 0.651*\text{BMRr}$$

As stated in Table 3, both regressors have a significant correlation with the response variable (*p-values*: mass = 0.0005; BMRr = 0.008). The diagnostic plots (shown in Fig. A1 in Appendix 1) do not highlight any major departure from the assumptions of the standard MLR model. Between the models considering all the species (which cannot include BMRr as regressor), the best one in terms of AIC and BIC has both ln (mass) and ln (long) as regressors; such model, has been refitted excluding *equus ferus caballus* and *gorilla*. In this way, it was comparable with the model containing ln (mass) and BMRr as regressors: AIC and BIC suggest that the model without BMRr and with ln (long) as regressor is sharply worse.

This model has been extended by performing a phylogenetic regression, as described in Section "Statistical analysis". The optimal value of the Pagel λ is 0, meaning that the best model is the one whose residuals do not reflect any phylogenetic signal. The log-likelihood function of the phylogenetic

Table 3 The summary of the main regression models on PD fitted on the data. The models flagged with a star are the ones disregarding some species to allow the inclusion of BMRr as a regressor, or to be comparable with the models considering BMRr. Among those, the best model is the one with mass and BMRr as regressors. The AIC and BIC values show that excluding BMRr and/or including longevity as regressors deteriorates the performance of the model. Based on AIC and BIC, the best model considering all the species (and so excluding BMRr from the analysis) is the one with mass and longevity as regressors.

Model (all species)	Explanatory variables + T-test *p-values*	AIC	BIC
Mass + Long	*ln(mass) - 0.002; ln(long) - 0.075*	20.37	23.20
Mass	ln (mass) - 0.0001	22.49	24.61
Model*	**Explanatory variables + T-test *p-values***	**AIC**	**BIC**
*Mass + BMRr**	*ln(mass) - 0.0005; BMRr - 0.008*	12.66	14.92
Mass + Long + BMRr*	ln (mass) - 0.002; BMRr - 0.039; ln (long) - 0.829	14.59	17.42
Mass + Long*	ln (mass) - 0.007; ln (long) - 0.122	19.08	21.34
Mass*	ln (mass) - 0.002	20.33	22.03
Model (phylo)	**Explanatory variables + T-test *p-values***	**AIC**	**BIC**
Mass + BMR* $\lambda = 0.10$	ln (mass) - 0.0006; BMRr − 0.009	12.89	15.15
Mass + BMR* $\lambda = 1.00$	ln (mass) - 0.018; BMRr − 0.118	21.32	23.58

Table 4 The summary of the main regression models on IF fitted on the data. The models flagged with a star are the ones disregarding some species to allow the inclusion of BMRr as a regressor, or to be comparable with the models considering BMRr. On both the settings of observations under analysis, the t tests and F tests clearly indicate that the model with only mass as regressor is the best one.

Model (all species)	Explanatory variables + T-test *p-values*	F-statistics (*p-value*)
Mass	*ln(mass) - 0.004*	*44.32 (0.00001)*
Mass + Long	ln (mass) - 0.021; ln (long) - 0.725	17.03 (0.0002)
Model *	**Explanatory variables + T-test *p-values***	**F-statistics (*p-value*)**
*Mass**	*ln(mass) - 0.006*	*36.55 (0.00004)*
Mass + BMRr*	ln (mass) - 0.013; BMRr - 0.798	14.69 (0.0006)
Mass + Long*	ln (mass) - 0.026; ln (long) - 0.733	14.03 (0.0007)
Mass + Long + BMRr*	ln (mass) - 0.034; BMRr - 0.953; ln (long) - 0.819	8.42 (0.003)

model for values of Pagel λ ranging from 0 to 1 is shown in Appendix 1 (Fig. A3).

Immortalization probability

Results of the MLRs with IF as dependent variable are summarized in Table 4. Based on the t-tests, no other independent variable is correlated with IF when controlling for the mass, so the best model is the one that includes only ln (mass) as regressor. The estimated regression equation is:

$$IP = \frac{1}{1 + e^{-[7.644 - 0.956 * \ln(mass)]}}$$

Figure. 4 shows the scatter plot of the log-transformed body mass and the observed immortalization frequency, as well as the fitted regression line. The diagnostic plots (Fig. A2 in Appendix 1) highlight, as it is already deducible from the scatter plot, that *mus musculus* has a notably high standardized residual.

This model has been extended by performing a phylogenetic regression considering only ln (mass) as explanatory variable. The optimal value of the Pagel λ for the model is 0, meaning that allowing for a correlation structure reflecting the phylogenetic relation between the species does not improve the regression model. The log-likelihood function of the phylogenetic model for values of Pagel λ ranging from 0 to 1 is shown in Appendix 1 (Fig. A4).

Discussion and conclusions

The relationship between replicative senescence and in vivo ageing has been widely studied. Initial smaller studies reported an inverse correlation between replicative capacity in culture and donors' age however this correlation was not reproduced in subsequent larger studies [21,27,28], reviewed by Lorenzini & Maier [29].

Regarding the correlation between replicative capacity and maximum species longevity, less evidence is available. Stanley et al. [30] did not observe a correlation, while Röhme [26], reported a clear relationship between the maximum lifespan of mammalian species and the lifespan of their fibroblasts and erythrocytes in vivo. In the latter study, data from embryonic and adult donors, which are known to differ in terms of proliferative potential, were combined. Our later study [18], resolved this apparent contradiction reporting that proliferative capacity is correlated with body mass and the apparent correlation with longevity is only a consequence of the known relationship between lifespan and body mass. The present analysis includes additional data to the 2005 report,

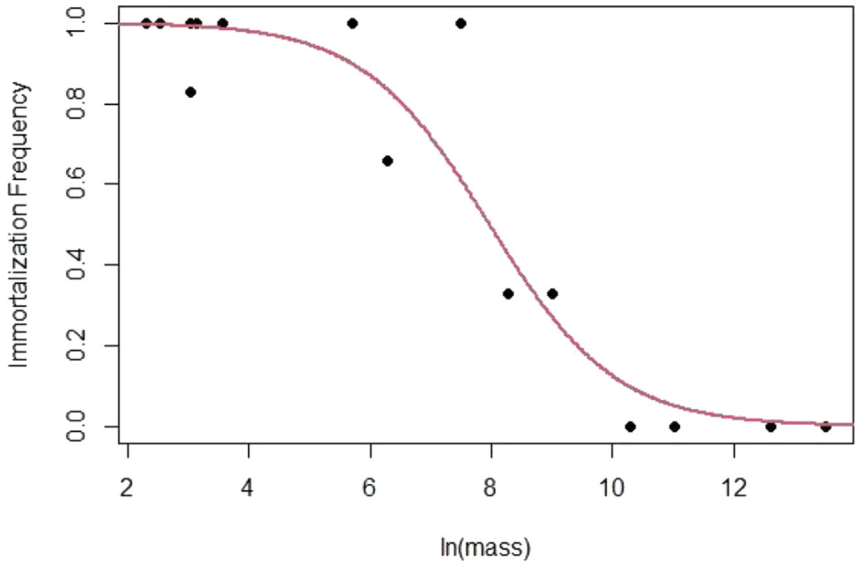

Fig. 4 Scatterplot of the log-transformed mass and observed immortalization frequency (IF), with the estimated regression line. The data points are generally close to the regression line. It is possible to observe that only one of the species with ln (mass) < 6 has an IF lower than 1 (mus musculus), while among the species with IF = 1 the highest ln (mass) is 7.50 (oryctolagus cuniculus).

confirming its results and strengthening the conclusions. Moreover, the present analysis suggests the presence of a relation between the basal metabolic rate (here expressed as BMRr) and the proliferative capacity, which could help in furtherly explaining the interspecies variability in terms of proliferative potential.

The correlation between proliferative potential and body mass is consistent with the fact that the number of cells of an individual is greater for larger species considering the modest variation in cell volume. Consequently, larger species must be equipped by natural selection with higher replicative potential. Regarding the correlation with BMRr we can just comment that a relationship between metabolic rate and replicative potential has been already proposed by Gillooly et al. [31].

Our analysis also brings a comparative view to the phenomenon of spontaneous immortalization. The analysis shows that the immortalization probability of the cell strains is not correlated with species longevity although it is correlated with species body mass. Following the accepted paradigm that cancer results from an accumulation of oncogenic mutations [32], immortalization is considered a key step toward transformation. Our observations do not support a connection between lifespan and cellular mechanisms for cancers avoidance but do support a connection between such mechanisms and the total number of cells of an individual. This is coherent with the fact that among the individuals of the same species, size is positively related to cancer risk [33].

A recent study has shown that longevity is correlated with mutation rate, while mass is not [17], this observation is consistent with our previous data documenting a correlation with the NHEJ [13]. Interestingly, in the present study, we found that longevity is not correlated with immortalization frequency, while mass is. One possible conclusion is that the evolution of large body mass required specific protection in order to limit the negative consequences of mutations accumulating in onco-suppressor genes and their regulatory regions. Supporting this hypothesis is the observation of the high copy numbers (20–40) of potentially functional p53 pseudogenes observed in elephants [34]. This amplification probably represents a strategy to reduce the risk of accumulating inactivating mutations on key protective genes. Spontaneous immortalization, at least in a subset of species, can be regarded as a phenomenon revealing the likelihood of cell cycle control failure because of genetic instability. Another potential mechanism could be the decreased telomerase activity observed by Gomes et al. in large species [35]; as described in the introduction, moreover, we observe a negative correlation between body mass and micronuclei frequency [11] and between body mass and spindle assembly checkpoint tolerance [12]. These studies suggest that the fidelity with which chromosomes are segregated in daughter cells during mitosis is particularly relevant in large species, where mitoses are numerous and where a disordered segregation will lead to aneuploidy, inducing genetic instability and potentially cancer or, in the case of our study, simply a greater chance for immortalization.

Another possible interpretation of our data, that is not mutually exclusive with the preceding hypothesis, is that replicative senescence is not a universal phenomenon. An observed senescent plateau of the cumulative growth curve of a cell strain in culture could result from a suboptimal culture environment. This second consideration is at least supported for several species of rodents in culture [36] and potentially hematopoietic cells in mice [37].

A recent analysis of zoos' pathological records has confirmed Peto's paradox in mammals [16]. This suggests that both large species and long-lived species have developed defense mechanisms against cancer. Despite this, we find out that only mass is positively correlated with proliferative capacity and negatively with immortalization frequency.

We note limitations to our study in terms of species number and number of individual replicates, and the fact that our observation is focused on only one cell type: skin fibroblasts. The evolution of longevity could require specific adaptations visible in other cell types. For example, astrocytes seem to display a shorter proliferative lifespan than skin fibroblasts [38] and tissue-specific stem cells respond differentially to DNA damage [39]. It cannot be excluded that other analyses, mirroring ours but performed on different cell types, could uncover different relationships among the investigated quantities.

We believe that our observation adds to the understanding of the complex phenomenon of cancer and that, in the future, the potential of comparative analysis must be further exploited through additional observations, especially those using cancer-resistant animal models. Comparative biology has the potential to show important biological relationships, such as the inverse link between developmental rate and longevity [40–42] that are undetected in studies of individual animal models.

Declaration of competing interest

All authors have no conflicts of interest.

Acknowledgments

Naked mole-rat skin biopsies were provided by Rochelle Buffenstein (Calico Life Sciences LLC). Squirrel skin biopsies were provided by Michael A. Steele (Wilkes University, Wilkes-Barre, PA). Big brown bat skin biopsies were provided by Anja Brunet Rossinni (Santa Clara University, CA). Deer mouse biopsies were provided by Deborah Kristan (California State University, San Marcos, CA). Cat biopsies were provided by Veronika Kiklevich (University of Alabama at Birmingham, AL). We are also grateful for help with cell culture from Theresa Marinucci, Mantao Liu, Lan Te, Bethanie White, Lindsey Lewis, and Valentina Barba and to Ulana Prociuk for help with karyotyping. Supported by USPHS grants AG20955, AG022873, and by the Mars Foundation to Vincent Cristofalo and by RFO MIUR Grants to AL.

Appendix A. Supplementary data

Supplementary data to this article can be found online at https://doi.org/10.1016/j.bj.2023.100596.

Appendix B - Aggregated data and code for statistical analysis

A GitHub repository containing the aggregated data from the cell strains and the R code to reproduce the analysis can be found at the following link: https://github.com/matteo-perillo/Interspecies-cell-immortalization-and-proliferative-capacity.

REFERENCES

[1] Hayflick L, Moorhead PS. The serial cultivation of human diploid cell strains. Exp Cell Res 1961;25(3):585–621.
[2] Baker DJ, Wijshake T, Tchkonia T, LeBrasseur NK, Childs BG, van de Sluis B, et al. Clearance of p16Ink4a-positive senescent cells delays ageing-associated disorders. Nature 2011;479(7372):232–6.
[3] Childs BG, Gluscevic M, Baker DJ, Laberge R-M, Marquess D, Dananberg J, et al. Senescent cells: an emerging target for diseases of ageing. Nat Rev Drug Discov 2017;16(10):718–35.
[4] Muñoz-Espín D, Cañamero M, Maraver A, Gómez-López G, Contreras J, Murillo-Cuesta S, et al. Programmed cell senescence during mammalian embryonic development. Cell 2013;155(5):1104–18.
[5] Demaria M, Ohtani N, Youssef SA, Rodier F, Toussaint W, Mitchell JR, et al. An essential role for senescent cells in optimal wound healing through secretion of PDGF-AA. Dev Cell 2014;31(6):722–33.
[6] Attaallah A, Lenzi M, Marchionni S, Bincoletto G, Cocchi V, Croco E, et al. A pro longevity role for cellular senescence. Geroscience 2020;42(3):867–79.
[7] Tosato G, Cohen JI. Generation of epstein-barr virus (EBV)–Immortalized B cell lines. Curr Protoc Im 2007;76.
[8] Irfan Maqsood M, Matin MM, Bahrami AR, Ghasroldasht MM. Immortality of cell lines: challenges and advantages of establishment. Cell Biol Int 2013;37(10):1038–45.
[9] Hanahan D, Weinberg RA. Hallmarks of cancer: the next generation. Cell 2011;144(5):646–74.
[10] Croco E, Marchionni S, Storci G, Bonafè M, Franceschi C, Stamato TD, et al. Convergent adaptation of cellular machineries in the evolution of large body masses and long life spans. Biogerontology 2017;18(4):485–97.
[11] Croco E, Marchionni S, Lorenzini A. Genetic instability and aging under the scrutiny of comparative biology: a meta-analysis of spontaneous micronuclei frequency. Mech Ageing Dev 2016;156:34–41.
[12] Lorenzini A, Fink LS, Stamato T, Torres C, Sell C. Relationship of spindle assembly checkpoint fidelity to species body mass, lifespan, and developmental rate. Aging 2011;3(12):1206–12.
[13] Lorenzini A, Johnson FB, Oliver A, Tresini M, Smith JS, Hdeib M, et al. Significant correlation of species longevity with DNA double strand break recognition but not with telomere length. Mech Ageing Dev 2009;130(11–12):784–92.
[14] Croco E, Marchionni S, Bocchini M, Angeloni C, Stamato T, Stefanelli C, et al. DNA damage detection by 53BP1: relationship to species longevity. J Gerontol A Biol Sci Med Sci 2017;72(6):763–70.
[15] Peto R, Roe FJ, Lee PN, Levy L, Clack J. Cancer and ageing in mice and men. Br J Cancer 1975;32(4):411–26.
[16] Vincze O, Colchero F, Lemaître J-F, Conde DA, Pavard S, Bieuville M, et al. Cancer risk across mammals. Nature 2022;601(7892):263–7.
[17] Cagan A, Baez-Ortega A, Brzozowska N, Abascal F, Coorens THH, Sanders MA, et al. Somatic mutation rates scale with lifespan across mammals. Nature 2022;604(7906):517–24.
[18] Lorenzini A, Tresini M, Austad SN, Cristofalo VJ. Cellular replicative capacity correlates primarily with species body mass not longevity. Mech Ageing Dev 2005;126(10):1130–3.
[19] Cristofalo VJ, Charpentier R. A standard procedure for cultivating human diploid fibroblastlike cells to study cellular aging. J Tissue Cult Methods 1980;6:117–21.
[20] Pignolo RJ, Masoro EJ, Nichols WW, Bradt CI, Cristofalo VJ. Skin fibroblasts from aged fischer 344 rats undergo similar changes in replicative life span but not immortalization with caloric restriction of donors. Exp Cell Res 1992;201(1):16–22.

[21] Cristofalo VJ, Allen RG, Pignolo RJ, Martin BG, Beck JC. Relationship between donor age and the replicative lifespan of human cells in culture: a reevaluation. Proc Natl Acad Sci USA 1998;95(18):10614–9.
[22] de Magalhães JP, Costa J. A database of vertebrate longevity records and their relation to other life-history traits. J Evol Biol 2009;22(8):1770–4.
[23] O'Neill DG, Seah WY, Church DB, Brodbelt DC. Rottweilers under primary veterinary care in the UK: demography, mortality and disorders. Canine Genet Epidemiol 2017;4:13.
[24] Salt C, Morris PJ, Wilson D, Lund EM, German AJ. Association between life span and body condition in neutered client-owned dogs. J Vet Intern Med 2019;33(1):89–99.
[25] Kleiber M. Body size and metabolic rate. Physiol Rev 1947;27(4):511–41.
[26] Röhme D. Evidence for a relationship between longevity of mammalian species and life spans of normal fibroblasts *in vitro* and erythrocytes *in vivo*. Proc Natl Acad Sci USA 1981;78(8):5009–13.
[27] Goldstein S, Moerman EJ, Soeldner JS, Gleason RE, Barnett DM. Chronologic and physiologic age affect replicative life-span of fibroblasts from diabetic, prediabetic, and normal donors. Science (1979) 1978;199(4330):781–2.
[28] Smith JR, Venable S, Roberts TW, Metter EJ, Monticone R, Schneider EL. Relationship between in vivo age and in vitro aging: assessment of 669 cell cultures derived from members of the baltimore longitudinal study of aging. J Gerontol A Biol Sci Med Sci 2002;57(6):B239–46.
[29] Lorenzini A, Maier AB. Influence of donor age and species longevity on replicative cellular senescence. 2016. p. 49–70.
[30] Stanley JF, Pye D, Macgregor A. Comparison of doubling numbers attained by cultured animal cells with life span of species. Nature 1975;255(5504):158–9.
[31] Gillooly JF, Hayward A, Hou C, Burleigh JG. Explaining differences in the lifespan and replicative capacity of cells: a general model and comparative analysis of vertebrates. Proc Biol Sci 2012;279(1744):3976–80.
[32] Takeshima H, Ushijima T. Accumulation of genetic and epigenetic alterations in normal cells and cancer risk. NPJ Precis Oncol 2019;3:7.
[33] Choi YJ, Lee DH, Han K-D, Yoon H, Shin CM, Park YS, et al. Adult height in relation to risk of cancer in a cohort of 22,809,722 Korean adults. Br J Cancer 2019;120(6):668–74.
[34] Sulak M, Fong L, Mika K, Chigurupati S, Yon L, Mongan NP, et al. TP53 copy number expansion is associated with the evolution of increased body size and an enhanced DNA damage response in elephants. Elife 2016;5.
[35] Gomes NMV, Ryder OA, Houck ML, Charter SJ, Walker W, Forsyth NR, et al. Comparative biology of mammalian telomeres: hypotheses on ancestral states and the roles of telomeres in longevity determination. Aging Cell 2011;10(5):761–8.
[36] Seluanov A, Hine C, Bozzella M, Hall A, Sasahara THC, Ribeiro AACM, et al. Distinct tumor suppressor mechanisms evolve in rodent species that differ in size and lifespan. Aging Cell 2008;7(6):813–23.
[37] Soerens AG, Künzli M, Quarnstrom CF, Scott MC, Swanson L, Locquiao JJ, et al. Functional T cells are capable of supernumerary cell division and longevity. Nature 2023;614(7949):762–6.
[38] Bitto A, Sell C, Crowe E, Lorenzini A, Malaguti M, Hrelia S, et al. Stress-induced senescence in human and rodent astrocytes. Exp Cell Res 2010;316(17):2961–8.
[39] Blanpain C, Mohrin M, Sotiropoulou PA, Passegué E. DNA-damage response in tissue-specific and cancer stem cells. Cell Stem Cell 2011;8(1):16–29.
[40] Marchionni S, Sell C, Lorenzini A. Development and longevity: cellular and molecular determinants – a mini-review. Gerontology 2020;66(3):223–30.
[41] Lorenzini A, Stamato T, Sell C. The disposable soma theory revisited: time as a resource in the theories of aging. Cell Cycle 2011;10(22):3853–6.
[42] Lorenzini A, Sell C. Enhanced stress-induced senescence-response may increase species lifespan. Aging 2021;13(12):15694–6.